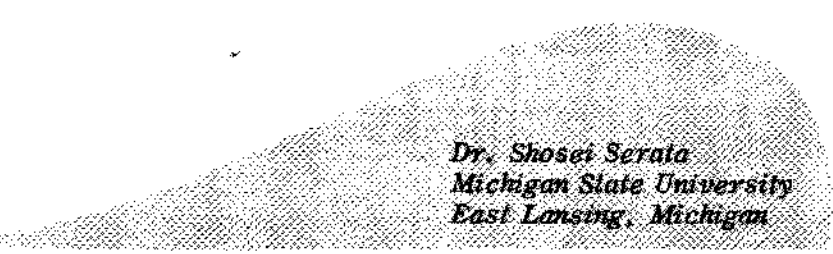


Continuum Theory and Model of Rock Salt Structures



Dr. Shosei Serata
Michigan State University
East Lansing, Michigan

ABSTRACT

The structural behavior of rock salt specimens tested in a laboratory appears to be quite different from that of actual salt mines. Furthermore, laboratory tests conducted by various investigators on the structural properties of rock salt have produced significantly different values. This paper reports on an effort to investigate the cause of these differences through extensive studies in the laboratory and the field. The structural behavior of rock salt was found to be consistent whenever the boundary condition of loading was identical. By treating salt mine structures as part of a continuous medium, the relationship of the structural behavior between the laboratory specimen and the salt mine was determined.

The behavior of an actual mine pillar is simulated by using a laboratory specimen and is therefore reproducible in the laboratory. The strength and creep characteristics of such a model pillar were studied. A similar model technique was developed for analysis of the openings. The behavior of a model cavity is related to that of an actual mine opening regardless of its opening form. The strain distribution around various openings was analyzed with respect to the initial stress condition in situ. The application of the model technique in evaluating the safety of an old mine as well as in the design of a new salt mine is discussed.

INTRODUCTION

The structural behavior of a given rock salt varies a great deal depending upon the testing conditions. Sometimes it flows like a viscous material; other times it cracks and crumbles. It was found through extensive laboratory and field work that the variation of behavior depends on the degree of confinement and, to a lesser degree, on strain hardening of the rock salt. Rock salt collected from various mines displays remarkably consistent structural properties under a given confinement condition.

The purpose of this discussion is first to define the properties of rock salt under confinement, and second, to illustrate the development and application of the laboratory model technique. The fundamental structural properties of rock salt are described in relation to the nature and degree of confinement. Based on the properties defined in the laboratory, the concept and application of the laboratory model technique of pillars and openings of salt mines are explained. The development and application of the creep-stress gage for direct determination of stress distribution in mine structures are discussed.

STRUCTURAL PROPERTIES

Friction Effects on Strength

The maximum strength of a salt block is significantly affected by its end friction condition. A large number of identical cubic specimens were crushed under two different end conditions, one

with and the other without the friction reducer. Those without the friction reducer consistently exhibited a strength twice that of the other. The two corresponding stress-strain curves illustrate the significance of the effects from the end friction condition in Fig. 1. The test result indicate a substantial reduction of the supporting strength of a mine pillar if there is a mud seam near the top or the bottom of the pillar. The reduction of strength is directly related to the effective friction coefficient of the mud seam. The effect of the mud seam may be eliminated either by altering the mining elevation or by increasing the cross section of the pillar.

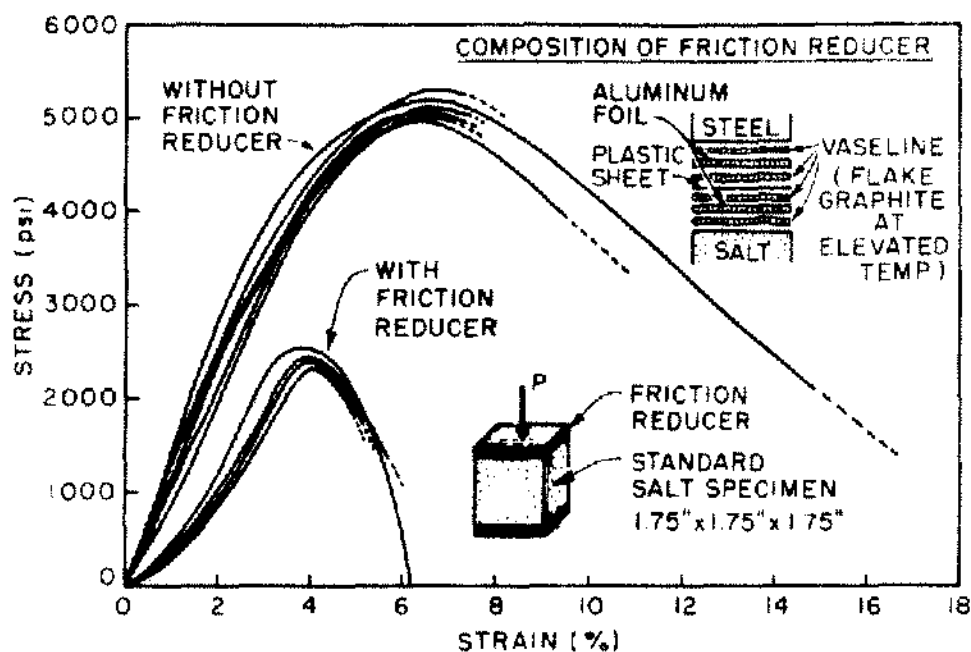


Figure 1. Effect of end friction reducer on stress-strain relation of rock salt.

Confinement Effect

In addition to the friction effect there is a significant effect of confinement to the mine structures due to the earth's lateral stress. In order to demonstrate the nature and the magnitude of this effect, four identical rock salt specimens were tested under four different confinement conditions as illustrated in Fig. 2. The two specimens, Types A and B, were compressed uniaxially; A with the friction reducer and B, without. The corresponding stress-strain curves are shown in the same diagram. Type C is a specimen identical to Type B except the height has been reduced to one half. The maximum strength has almost tripled the true strength. Type D is a specimen identical to Type C except it is laterally confined at both ends. This specimen cannot be crushed by loads up to 20,000 psi. The salt simply flows.

This test result may explain the reason for the large plastic flow observed in a deep salt mine. It also demonstrates the significant change in the supporting strength of a salt pillar by a change in the pillar design.

Brittle Failure and Ductile Flow of a Salt Pillar

The mechanism of the radical change in the pillar characteristics from brittle to ductile has been analyzed by using cylindrical specimens with the diameter of 3.25 inches. The four tested specimens are shown with their maximum strengths in Fig. 3. Both ends of the four specimens are confined by a pair of steel cylinders with friction conditions similar to the previous four specimens described which will be shown in Fig. 2. The failure of the first specimen at 2,500 psi is characterized by brittle failure of the grains, not the crystals. This corresponds to Type A. The

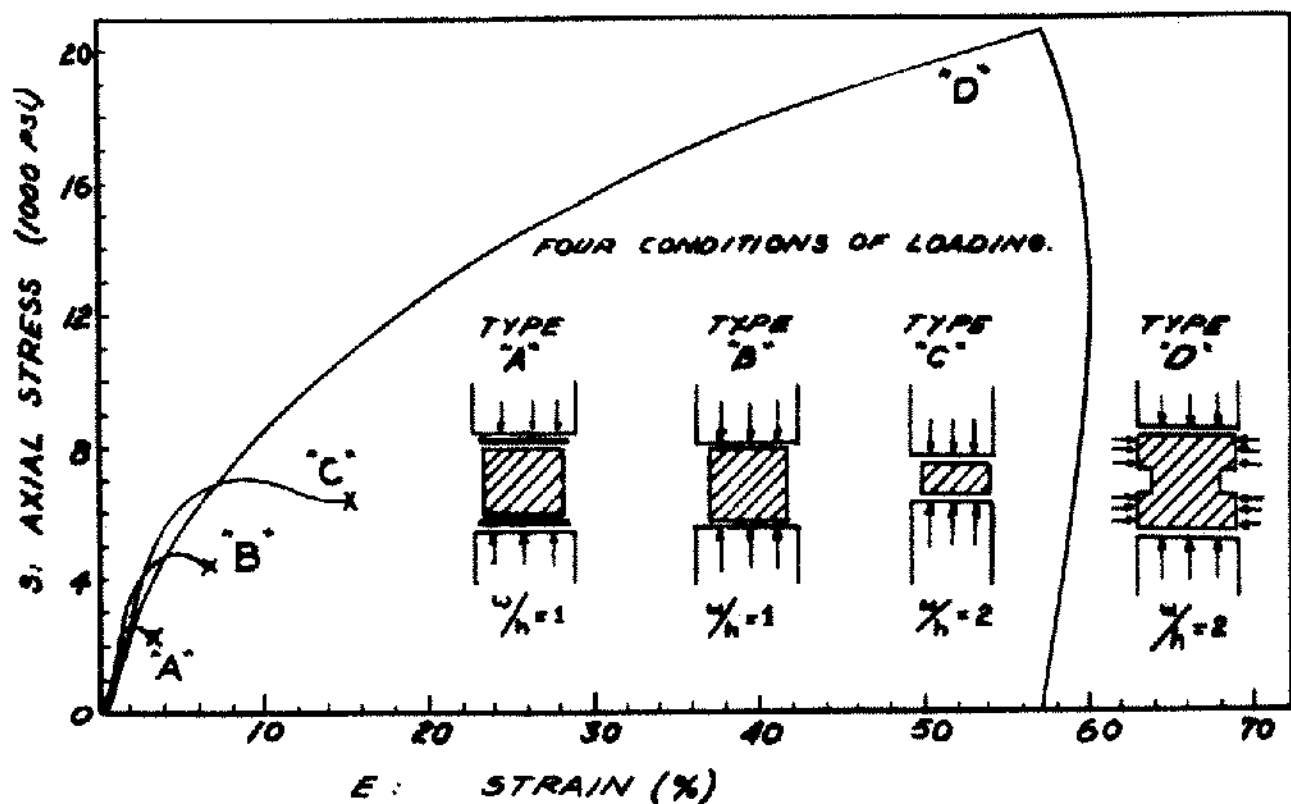


Figure 2. Effect of confinement upon behavior and strength of rock salt pillar.

failure of the second at 5,000 psi shows a pyramid of confined mass forming from both ends. Obviously, two quite different processes of deformation are involved here; one is brittle failure and the other, triaxial deformation. The triaxial deformation dominates the third pillar. The fourth pillar can withstand a vertical pressure of up to 20,000 psi. However, the steel cylinders will start to yield at this point.

The brittle failure is characterized by separation of the individual grains, and therefore the strength of the material is determined by the cohesive bonding among the grains. A study of this grain behavior is shown in Fig. 4. An important discovery of the test is that the increase of the triaxially compressed portion in a pillar increases the supporting strength of the pillar, and as the

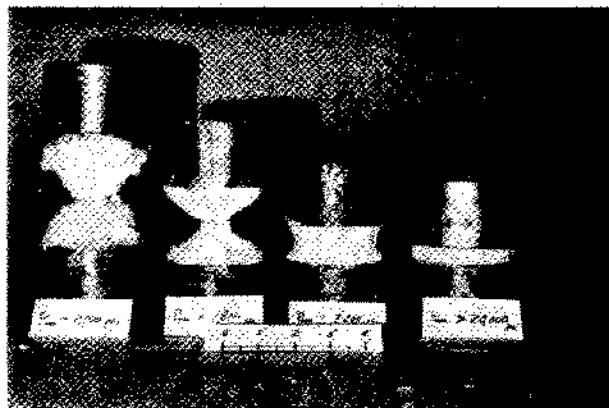


Figure 3. Failure pattern of salt pillar under various degrees of confinement demonstrating the two different processes of deformation.

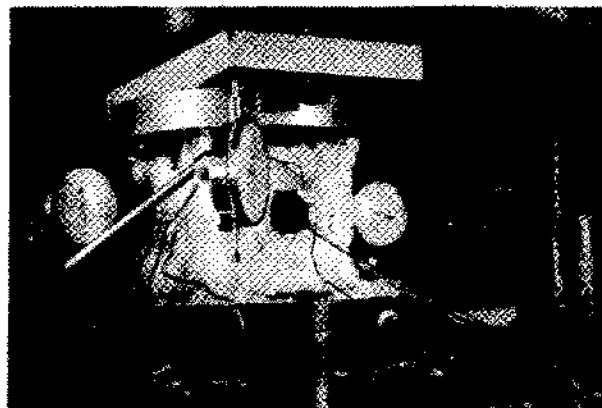


Figure 4. Laboratory observation of brittle failure and individual crystalline grain movement.

triaxially-compressed portion dominates the pillar medium, the pillar starts to flow with the brittle zone limited to the exposed surface. Thus, the supporting strength of a mining panel can be increased by a proper change in the panel design.

Transition Test

The triaxial deformation can be studied by using a new concept of a triaxial testing method, designated the transition test (Serata and Morrison, 1962). The testing method has been successfully developed in the laboratory as described in the following section. A schematic diagram of the transition test is presented in Fig. 5. This test was devised to study a confined medium (Sokolnikoff, 1956).

A specimen is tightly confined in a steel cylinder. Pressure is applied from the top and the corresponding stresses and strains in the three principal directions are measured. From this test the structural properties of the confined salt mass, such as, Young's modulus, E ; Poisson's ratio, ν ; octahedral shearing coefficient, G_1 ; retarded shear coefficient, G_2 ; viscoplastic coefficient, η_1 ; viscoelastic coefficient, η_2 ; and octahedral shearing strength, τ_0 , may be determined (Serata, Dahir, and others, 1964).

In Fig. 5 the lateral stress and the elastic coefficients of the test specimen are related to the applied stress, S_z , and the observed strains, e_v and e_h . (Serata, 1961 and 1964.)

A typical result of the transition test is shown in Fig. 6. This shows that the behavior of the confined continuous medium is entirely different from ordinary brittle behavior. An increase of the axial stress induces the lateral stress by reaction of the confinement which increases along the elastic line. A transition takes place suddenly at the point where the slope of the elastic line shifts to 45° . After reaching a certain point on the 45° line, the axial stress is reduced. Then, the lateral stress decreases along the elastic line, parallel with the initial elastic line. It reaches

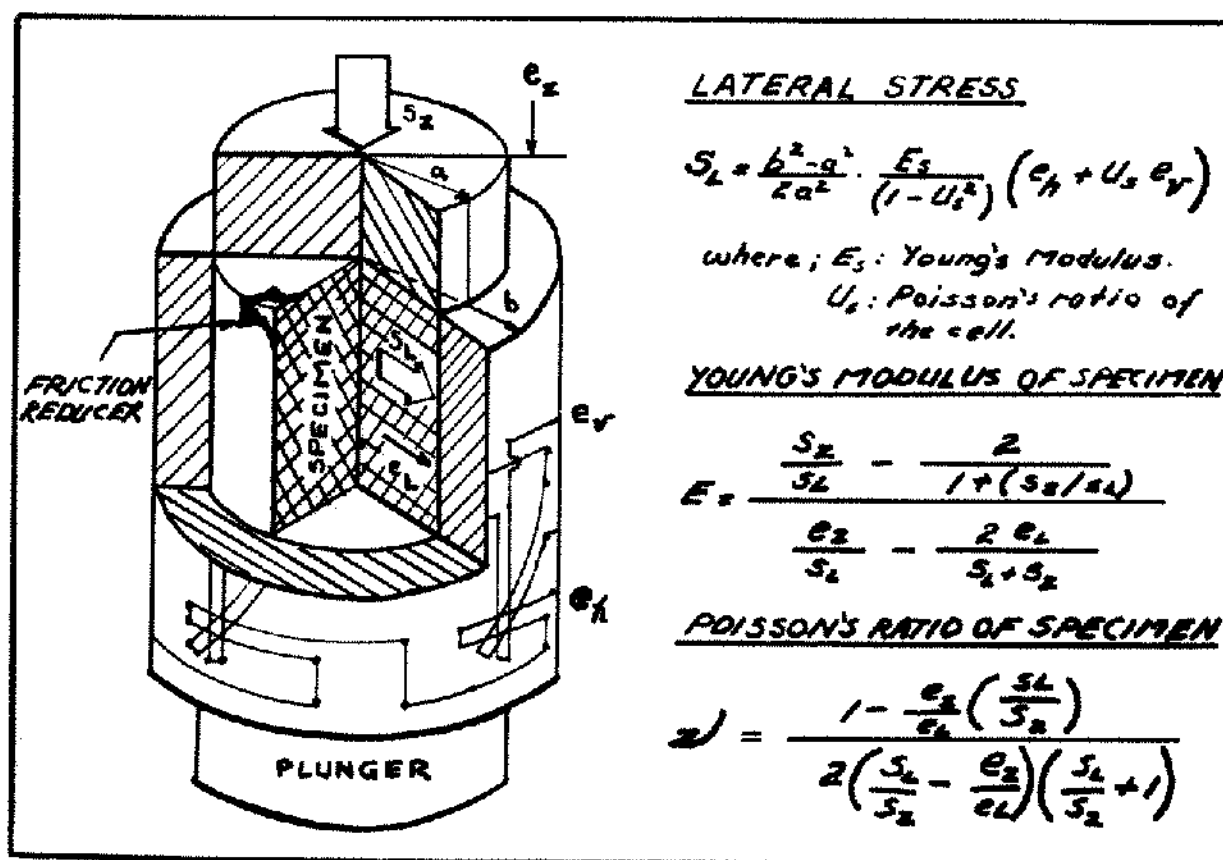


Figure 5. Cutaway view of specimen and cell of transition test and equations for basic parameters of tested material.

The graph plots lateral stress (S_2) against axial stress (S_1) for concrete under cyclic loading. The y-axis represents S_2 (LATERAL STRESS) in units of 1000 psi, ranging from 0 to 10. The x-axis represents S_1 (AXIAL STRESS) in units of 1000 psi, ranging from 0 to 14. Two data series are shown: the third cycle (solid line with open circles) and the fifth cycle (dashed line with solid circles). The graph is divided into regions: PLASTIC (top right), ELASTIC (bottom left), and HYDROSTATIC (center). A dashed line represents the octahedral shearing strength ($K_{sh} = 1500$ psi). Angles of 45°, 34°, and 44° are indicated. An inset diagram shows a cylindrical concrete specimen under triaxial stress with principal stresses S_1 , S_2 , and S_3 .

5

MODEL PILLAR

The results from the laboratory studies of the confined medium were utilized for evaluating the behavior of mine pillars. The laboratory results were condensed into a mathematical expression of the confined medium which is given in Fig. 8. Although the equations were established only for the confined medium, they can be usefully applied in the analysis of mine pillars as follows.

Model Pillar Concept

The usefulness of the equations were first tested in the laboratory and then confirmed by mine observations. The concept of a laboratory model of a mine pillar is illustrated in Fig. 9. A mining panel may consist of a repetition of the unit block which is illustrated in the figure. A model pillar analogous to the unit block is made of a five-inch cube as shown in Fig. 10. The model pillar is loaded to simulate the field condition and its creep behavior studied. The model pillars under creep loading are shown in Fig. 11.

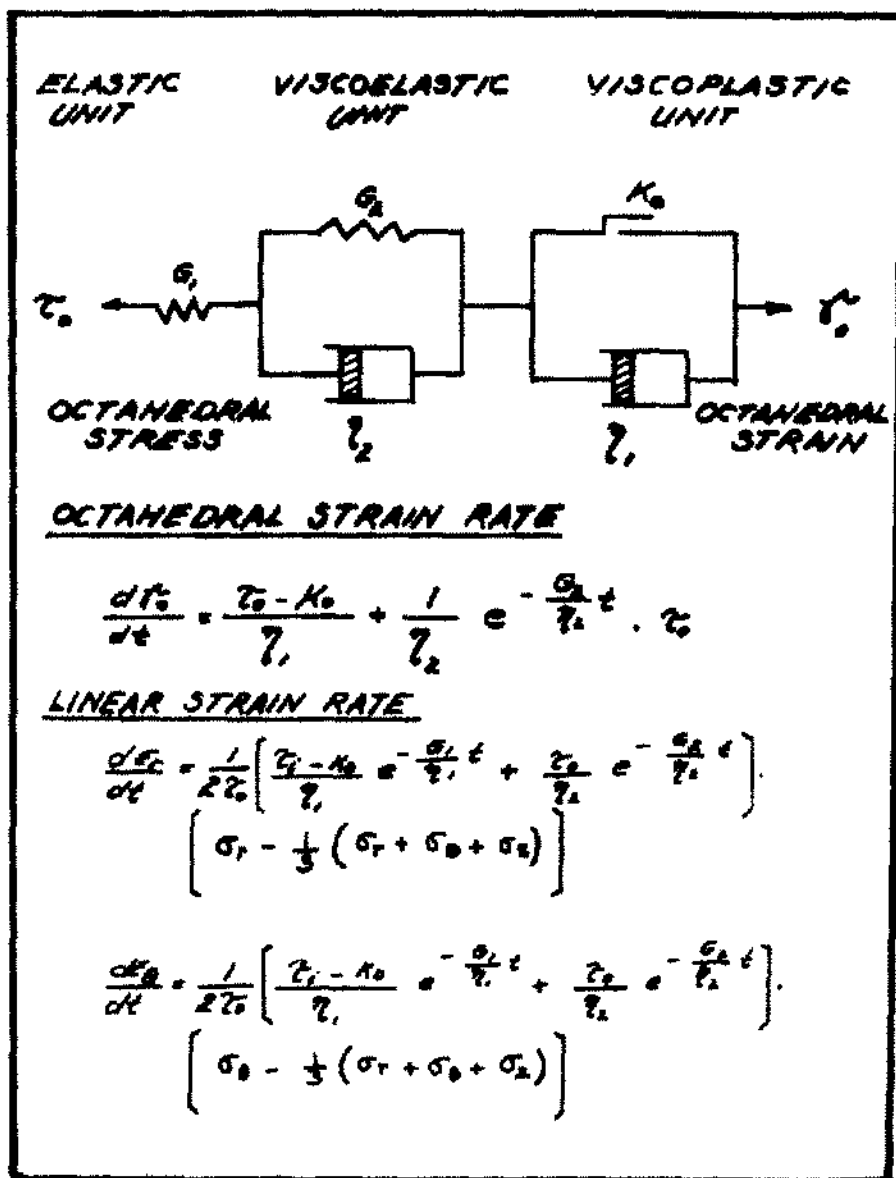


Figure 8. Mechanical model for confined medium of rock salt and mathematical expression of its behavior.

In the development of the model pillar the effect of the individual grains constituting the pillar has been analyzed theoretically, and the validity of the model technique verified in the laboratory. There are always four octahedral planes of yielding at any given point in the medium (Hill, 1960). The orientation of the principal stresses at the point changes along the circular wall of the pillar. This results in formulation of no specific yielding planes with respect to the crystal lattice direction of the crystal grains of the pillar. This theoretical conclusion that the crystal grains do not interfere with the model pillar behavior has been verified in the laboratory. A partial proof of this is observed in the brittle failure of the model wall as illustrated in Figs. 12, 13, and 14. The characteristics of the brittle failure of the wall surface is independent of the individual grain movement, and furthermore, they are quite similar to the brittle scaling on surfaces of pillars in salt mines (Serata and Gloyna, 1959).

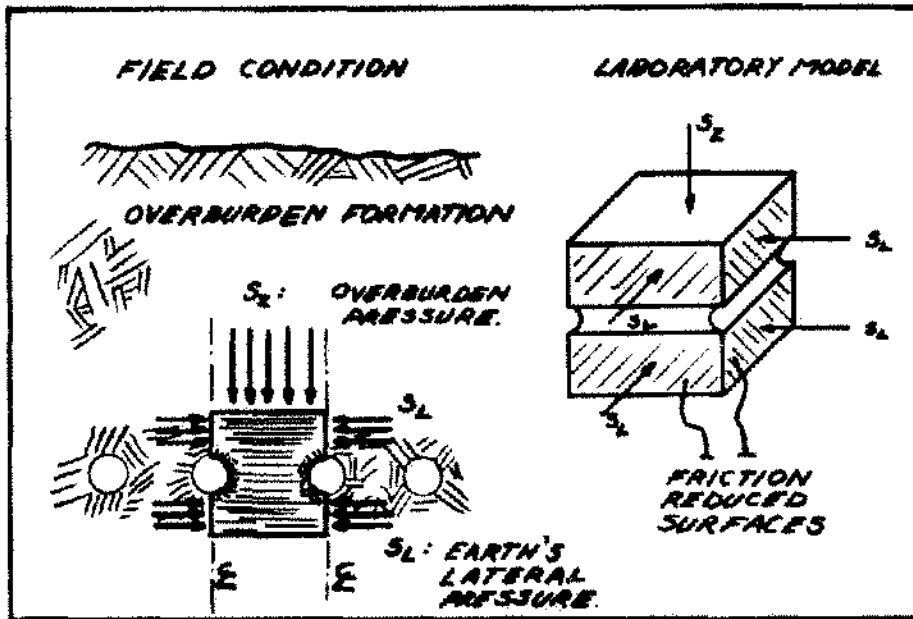


Figure 9. Conception of model of mine pillar representing unit block of mining panel.



Figure 10. Model pillar specimen showing proportion of the confined medium to the pillar.

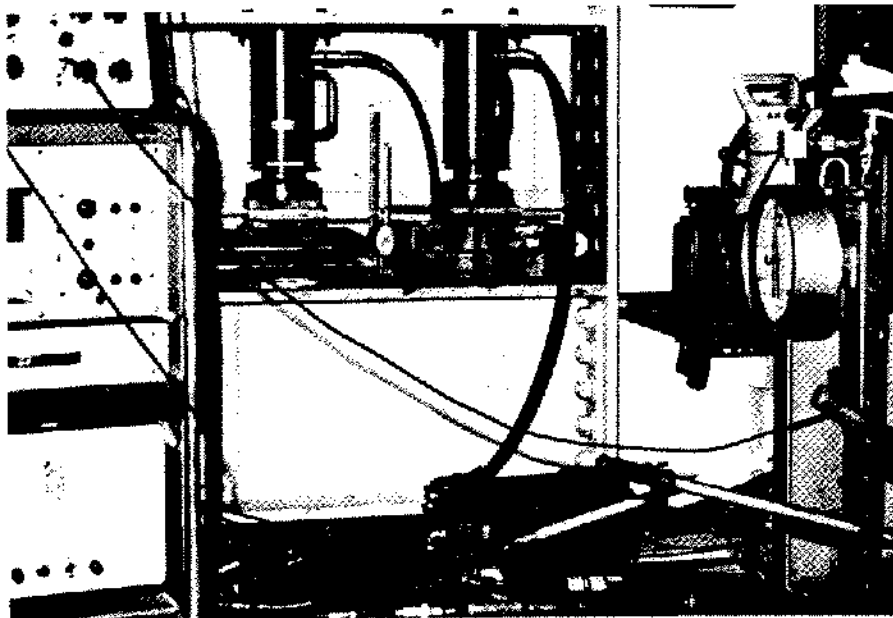


Figure 11. Laboratory setup for creep loading of model pillars.



Figure 12. Close-up of model pillar wall showing constitution of crystal grains.

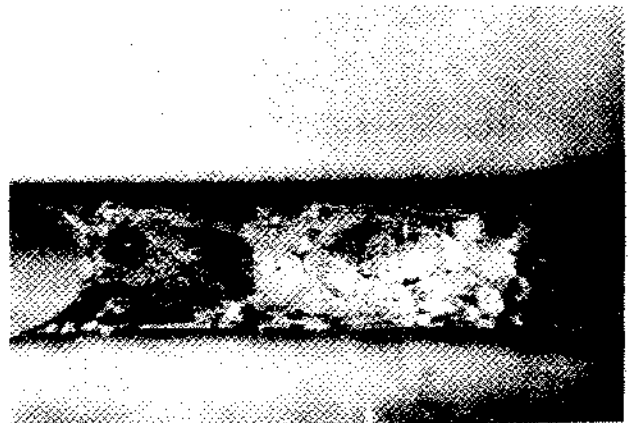


Figure 13. Model pillar after long-term creep deformation demonstrating brittle failure of wall is independent of crystal grains.

Laboratory and Field Results

The creep theory of the salt pillar was first tested with the laboratory model, and then, in various salt mines. In the laboratory the model was loaded vertically and the lateral pressure was provided by the steel confinement plates.

Two typical experimental results of the model pillar creep are compared in Fig. 15. The creep rate of the pillar is analyzed with respect to time of loading. Two parallel curves of creep rate are obtained from two different creep loads, 4,300 and 5,300 psi. Each curve of the total creep is separated into two straight lines of viscoelastic and viscoplastic flows. The coefficients of viscoelastic and viscoplastic flows determined from the slopes of these straight lines are in fair agreement with those obtained from the transition test.

It is significant that the creep of the pillar agrees with the theory of a confined continuous medium. This indicates that after elastic and brittle deformation, the creep behavior of the pillar

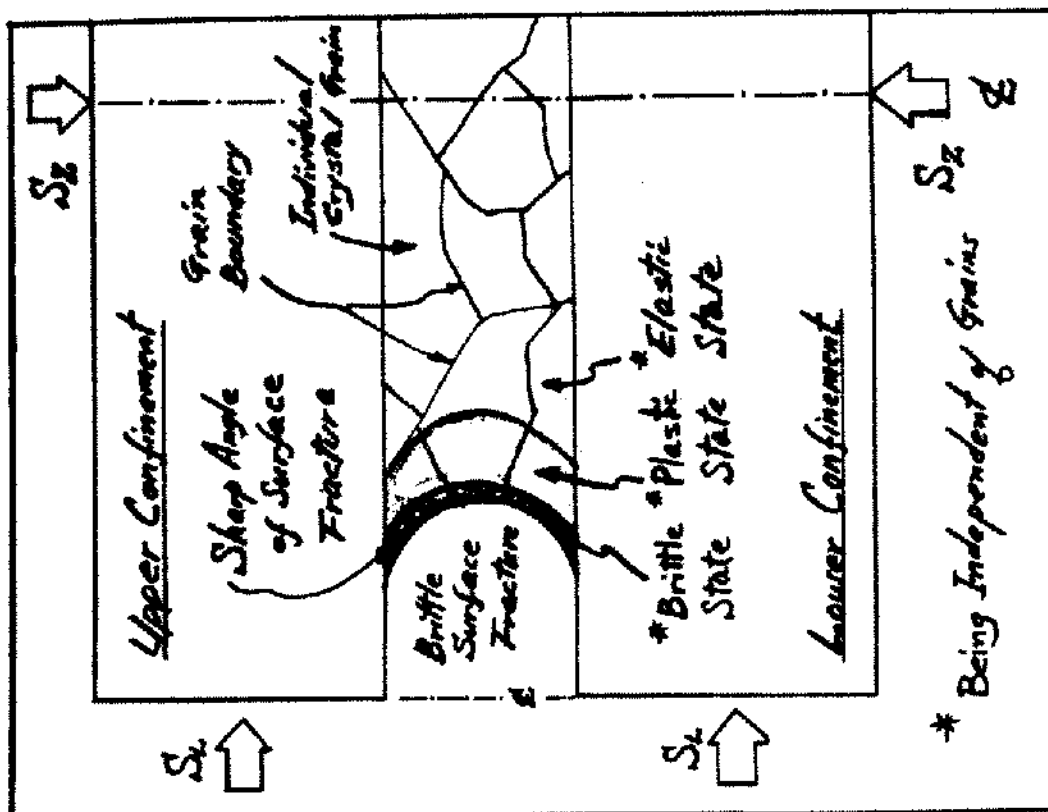


Figure 14. Analysis of stress state in model pillar simulating behavior of salt mine pillar.

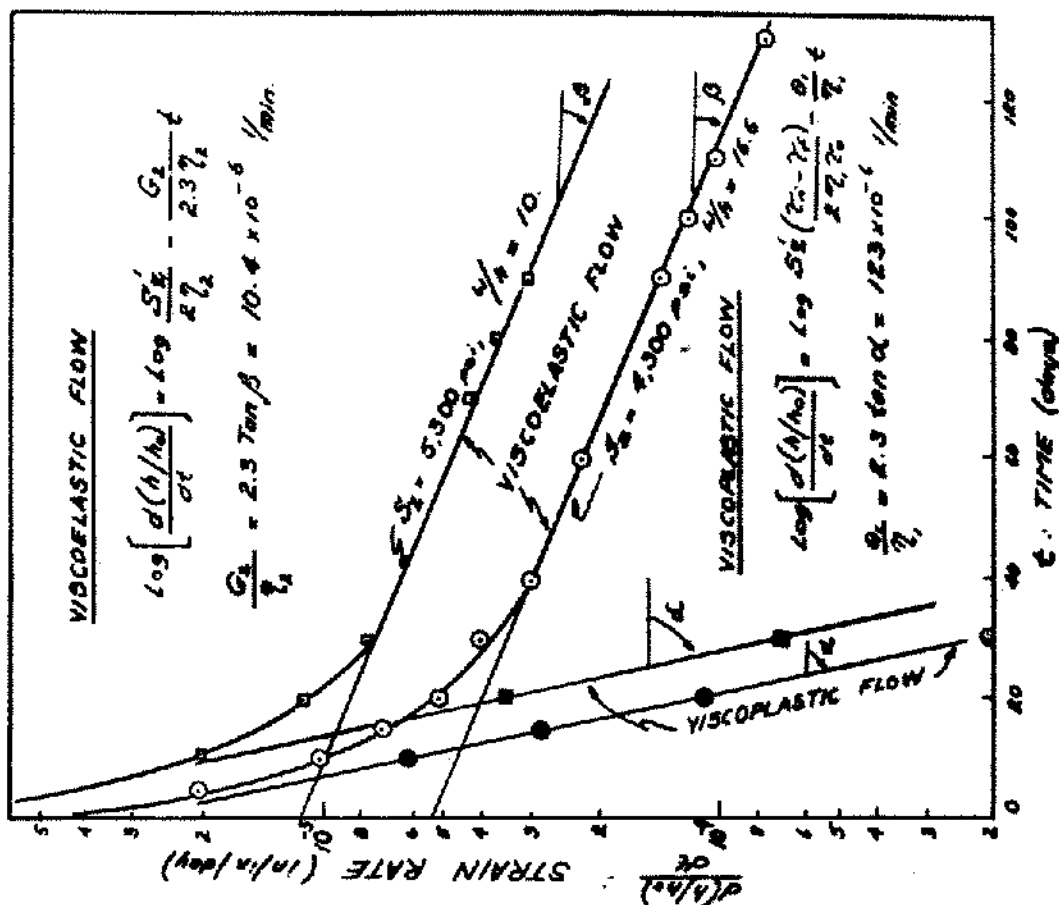


Figure 15. Separation of model pillar strain rate into two components of viscoplastic and viscoelastic flows.

is governed by the triaxially confined portion of the pillar. The creep behaviors of various mi pillars are in good agreement with their models. It has been proven that the creep rate of a g salt pillar is very closely related to its structural stability. In the design of a salt mine the c rate for a given mining panel can be predetermined by using the model technique. The laborat model technique has been applied in several salt mines for improving the supporting strength o pillars as well as determining the maximum extraction rate, given certain requirements for s tural safety.

MODEL OPENING

The concept of the laboratory model is further applied to openings in salt mines. First, validity of the model opening is verified by using a photoelastic method, and also through vari field measurements.

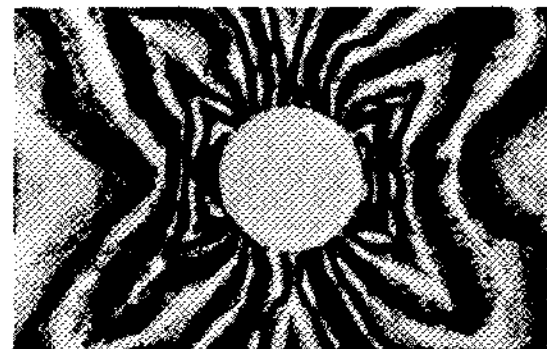
Photoelastic Analysis of Salt Cavities

The validity of the model salt cavity was tested by using a photoelastic technique. A pla type, birefringent sheet was attached on the surface of a five-inch cube specimen. A hole was drilled at the center of the sheet through the specimen. The deformation of the rock salt was lyzed on the surface by using the photoelastic method and was compared with the mathematica theory of cavity deformation. It has been shown that the behavior of the model cavity is close approximate to the theory (Chowdiah, 1963).

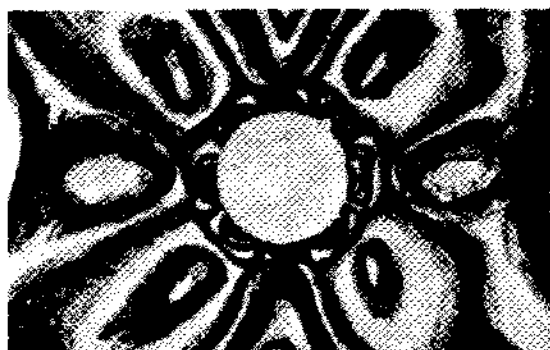
Some of the experimental results are shown in Figs. 16 to 18. Fig. 16a shows a photoe pattern which developed around a one-inch diameter opening in the standard five-inch cube sp men subjected to an equal biaxial pressure of 3,000 psi. This deformation pattern of rock sa



(a)



(b)



(c)

Figure 16. Photoelastic analysis of deformation around circular opening in rock salt: continuum demonstrating independence from grain effects and high sensitivity to the applied stress states,

clearly indicates agreement with the elastic-plastic theory of a circular opening (Serata and Dahir, 1964). The high intensity of the lines around the opening boundary indicates the plastic zone. The irregularity of some of the fringe lines is due to an irregular movement of individual grains of the specimen. Nevertheless, it is obvious that the effect of the grain movement upon the overall behavior of the cavity is insignificant.

Sensitivity of the model cavity may be demonstrated by the change in the birefringent pattern as the lateral stress is reduced to 1,000 psi while the vertical stress is maintained at 3,000 psi as shown in Fig. 16b.

Further reduction of the lateral stress to zero produces the pattern of uniaxial compression as shown in Fig. 16c. The behavior of a square opening in rock salt was examined under the equal biaxial pressure of 3,000 psi as shown in Fig. 17. Formation of the stress arch is seen around the roof as well as the wall. A wider opening with the equal biaxial pressure of 3,000 psi is shown in Fig. 18. The development of the stress arch is very pronounced over the roof while a highly plastic area develops around the walls.

Model Study of a Deep Mine

The biaxial loading condition of the model becomes inadequate as the applied pressure exceeds 3,000 psi. For such conditions the third principal stress direction must be confined. This means that a completely triaxial loading condition is required for study of salt mines at depths greater than 3,000 psi.

To provide a completely triaxial loading condition, a new triaxial testing machine was required with the following qualifications. First, the machine should have individual control of pressure in each of the three principal stress directions; at the same time, the cavity made in a testing specimen should be accessible for measurement. Such a testing machine was constructed as shown in Fig. 19. The five-inch cube specimen is compressed from three principal directions and the deformation of the cavity in the specimen is measured through a hole in the back plunger plate. An automatic pressure regulating system for operation of the testing machine is shown in Fig. 20 which includes automatic pumps, hydraulic shock absorbers, and safety control gages. The unique ability of this machine is to provide any desired control and measurement of all the principal stresses and strains which cannot be accomplished by the ordinary triaxial testing machine.

Analysis of Circular Opening

The time-dependent closure rate of a circular opening is analyzed in Fig. 21. Similar to the pillar analysis, the total flow is separated into two straight lines in the semilog diagram, one for viscoelastic and the other, viscoplastic. The constants determined from the circular opening are

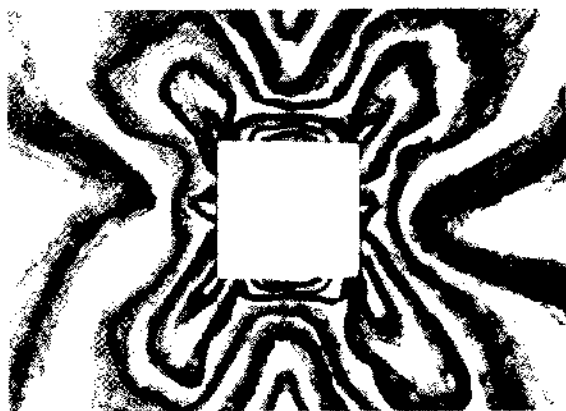


Figure 17. Photoelastic analysis of behavior of square opening made in rock salt medium under hydrostatic loading of 3,000 psi showing plastic zone developed at corners.

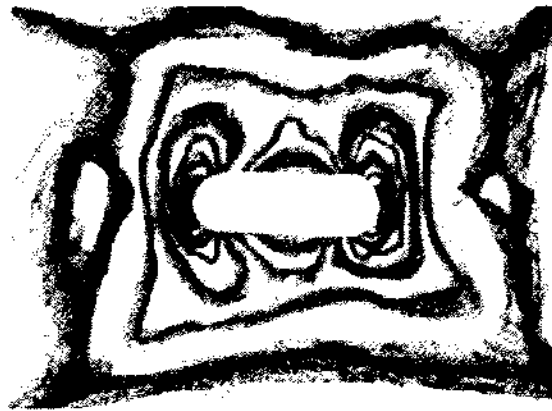


Figure 18. Photoelastic analysis of oval opening in rock salt under hydrostatic loading of 3,000 psi demonstrating plastic zones developed around circular wall and stress arches over the roof leaving brittle zones under the arch.

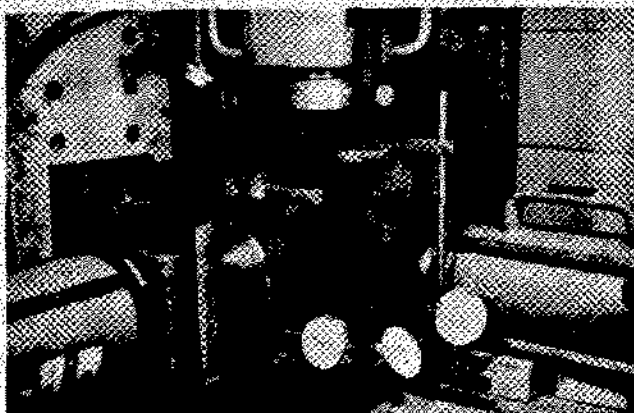


Figure 19. Triaxial testing machine with individual control of the three principal stresses for rock salt specimen of five-inch cube.

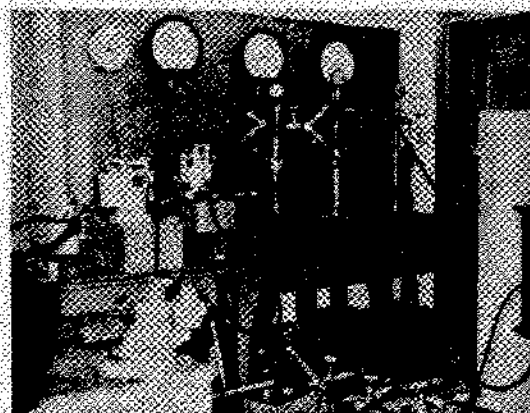


Figure 20. Automatic pressure regulating system for the control of the three principal stresses to be used for yield and long-term creep testing of rock salt.

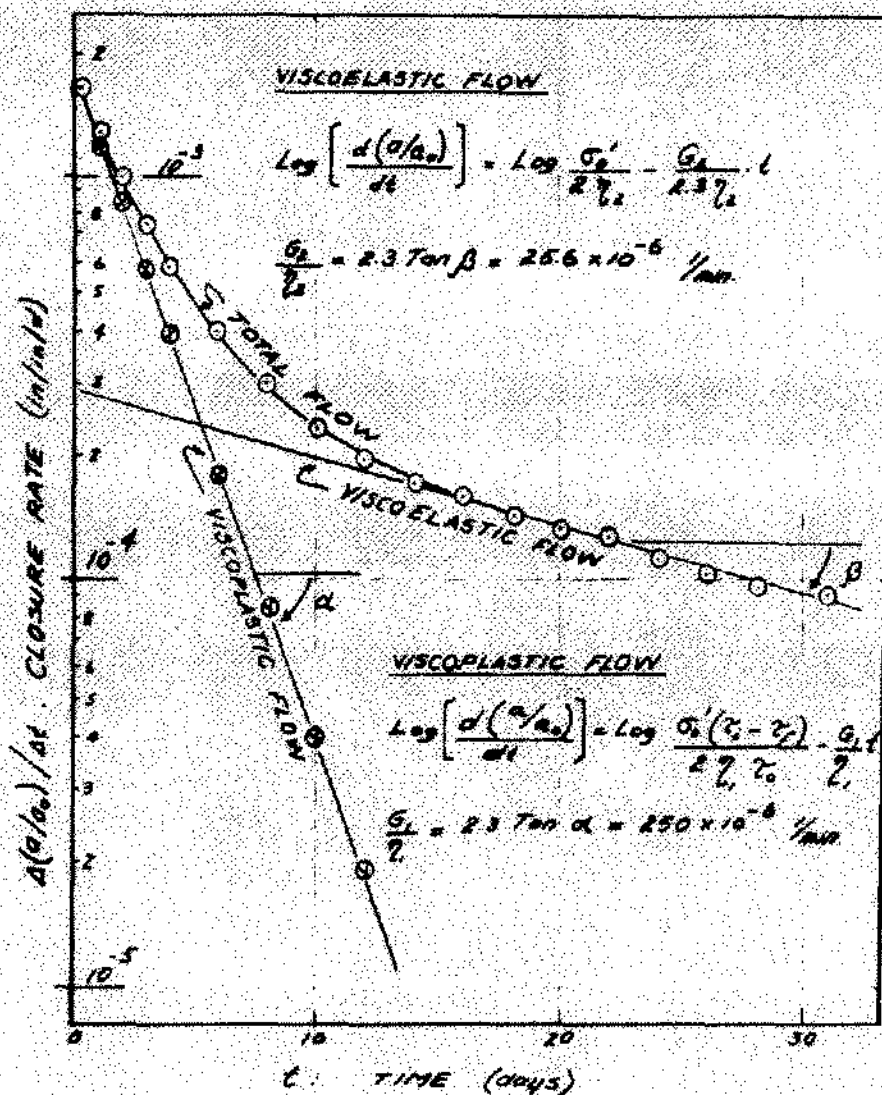


Figure 21. Analysis of metal cavity in rock salt medium confined by hydrostatic pressure of 3,000 psi.

in close agreement with the values obtained by the transition test. This again demonstrates that the creep of the opening is governed by the triaxially confined portion of the surrounding salt (Serata and Dahir, 1964).

Field Verification

A field measurement made in a circular opening in a deep salt mine was reported by Barron and Toews (Barron and Toews, 1963). The data given in the report was analyzed based on the theory of cavity creep which was developed in the laboratory. The graphical analysis of the field data was found to be in close agreement with the laboratory result of Fig. 21 regarding both magnitude and slope of the creep deformation.

SPECIAL APPLICATIONS

The laboratory model technique should find many immediate applications in salt mines. As a matter of fact, it has already been successfully applied in designing safe and economical salt mines. This study has also led to the development of a new stress gage. It was found from the models that the creep rate in a circular hole made in a confined continuous medium is related to the initial stress field of the medium. By using this relationship, a creep rate distribution measured in a drill hole can be used for determination of the stress field.

Stress Field Measurement

The first application of the creep-stress gage is illustrated in Fig. 22. A creep-stress gage was designed to measure the creep rate of a drill hole penetrating a salt formation at

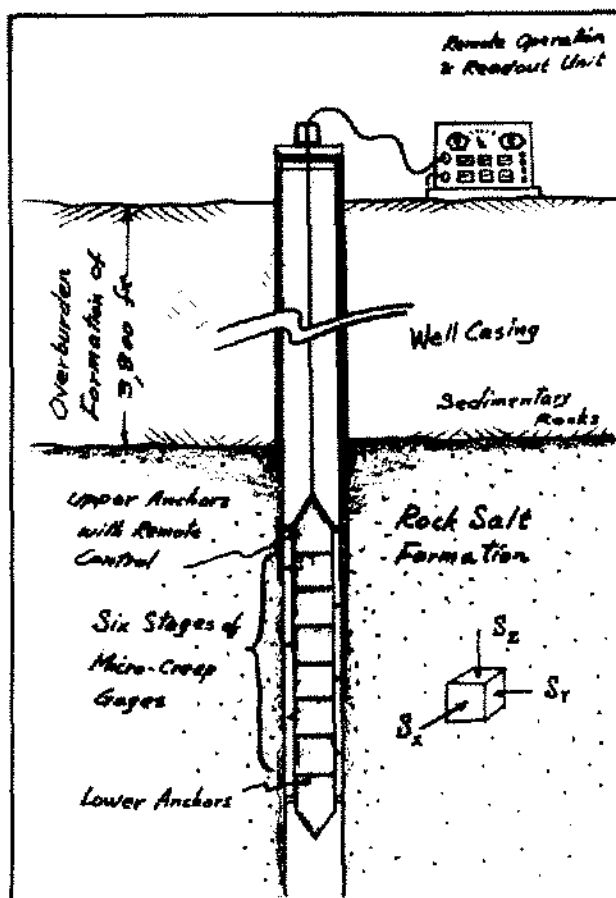


Figure 22. Application of creep-stress gage for determination of stress condition in rock salt formation from surface.

approximately 3,800 feet deep. The schematic diagram of the gage is shown in Fig. 23. This gage will be anchored at the desired depth, then six creep probes will be extended to the wall. The closure flow of the salt will continuously push the probes and the amount of the displacement will be transmitted to the recorder on the surface. The creep rate thus obtained will be used to calculate the stress field in the salt formation. This data in turn may determine the feasibility of mining the ore in this area.

Pillar Analysis

The creep-stress gage can also be used in operating mines to evaluate the safety of a mine pillar. Figure 24 shows a schematic diagram of such an operation. A typical salt pillar is shown with distribution of the axial and lateral stresses. The brittle zone of the pillar supports a very limited load. The plastic zone is characterized by the maximum stress difference between the vertical and lateral stresses. In the elastic state the stress difference is reduced from the maximum value. Installation and operation of the creep-stress gage would enable us to determine the stress distribution. The areal integration of the vertical stress will give us the acting load on the pillar.

Roof Analysis

A similar application may be made to evaluate the safety of the roof medium as illustrated in Fig. 25. The stress distribution in the roof is quite different from that of the pillar because the zone of the highest lateral stress lies at a certain depth from the roof surface. The magnitude of the stress concentration in the mass under the stress arch determines the structural competence of the roof.

Field Test

The first creep-stress gage developed in the laboratory was used by Dr. William James of the firm of James, Cooper and Buffam in an attempt to predetermine the stress field in a potash

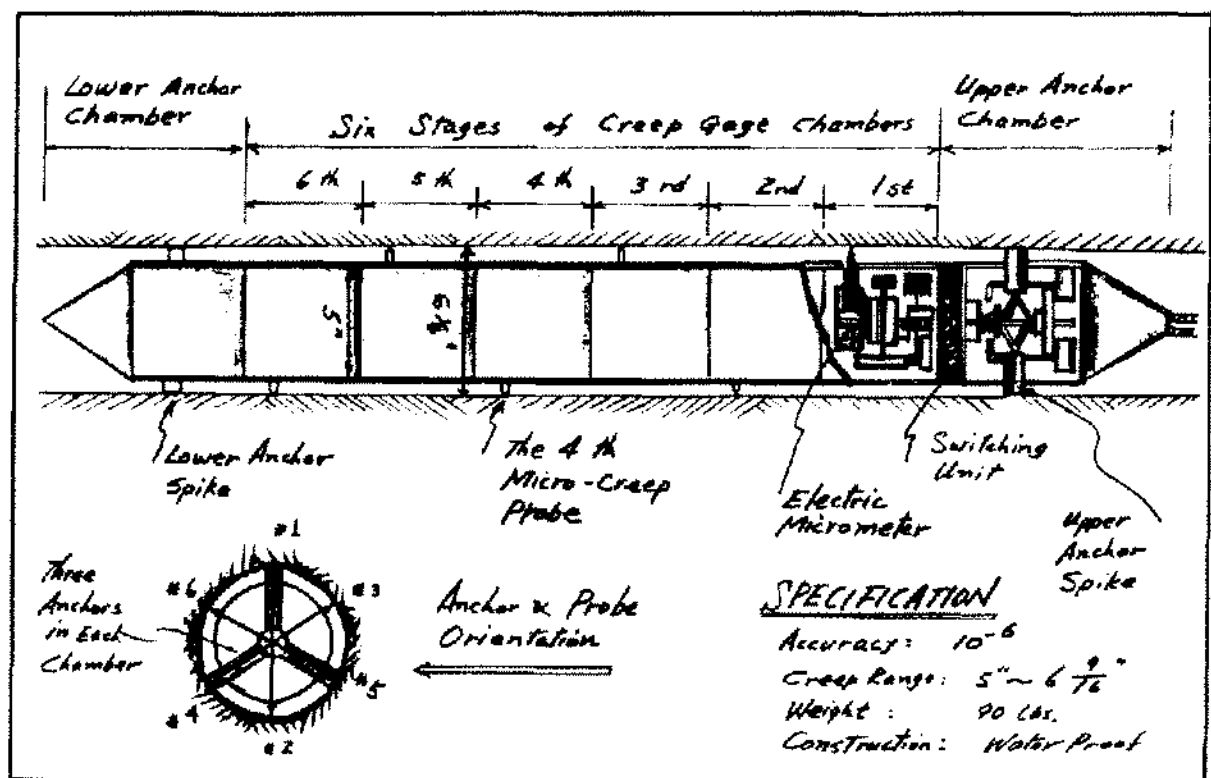


Figure 23. Schematic diagram of creep-stress gage.

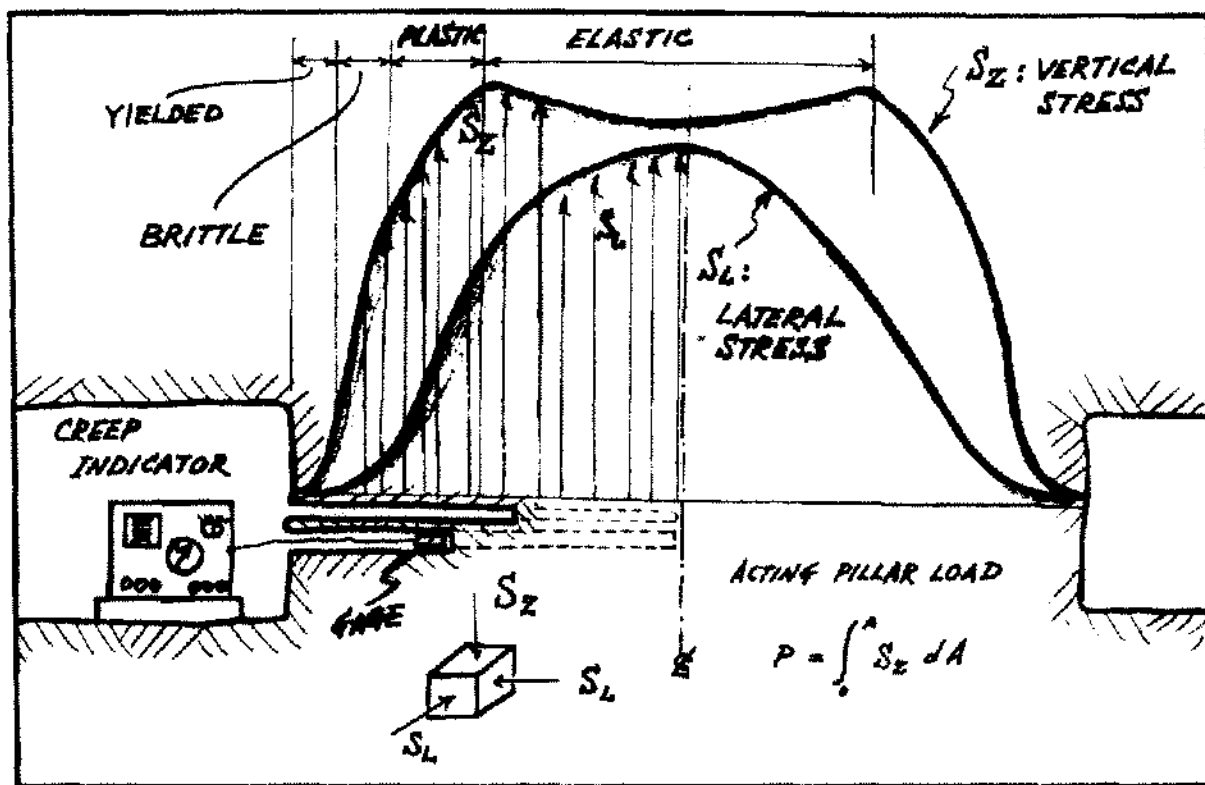


Figure 24. Measurement of stress distribution in mine pillar by using creep-stress gage.

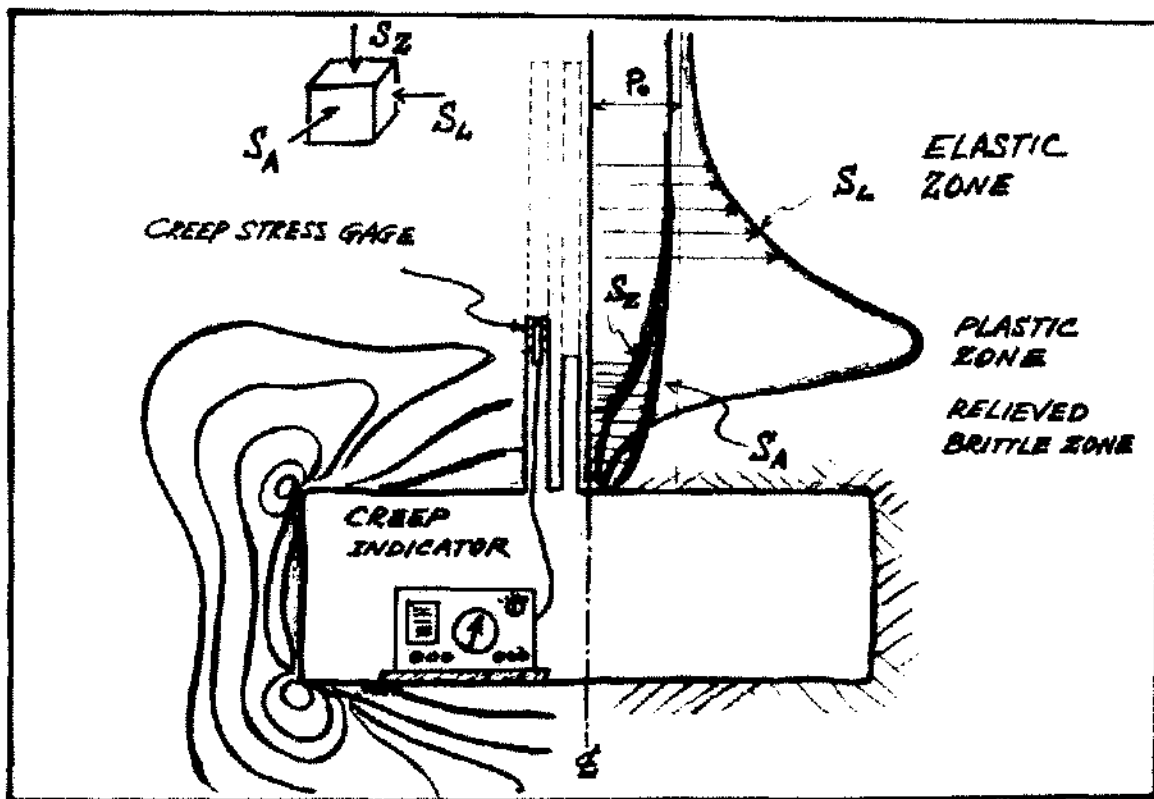


Figure 25. Measurement of stress condition in mine roof by using creep-stress gage.

deposit near Saskatoon, Canada. The gage which is shown in Fig. 23 was built with a capability of measuring closure displacement of the opening radius in six different directions in the plane perpendicular to the direction of the drilled hole. The six measurements can be made simultaneously with an accuracy of $\pm 1 \times 10^{-6}$ in./in.

The preliminary work of drilling and casing of the test hole is viewed in Fig. 26. The final checkup of the gage is shown in Fig. 27. The gage was sunk by using the drilled derrick as shown in Fig. 28. The remote control and readout unit is shown in Fig. 29. Although the test is still running, the preliminary analysis of the creep data obtained from this test indicates a general agreement with the theoretical prediction. A complete analysis of these field experiments will be made available in the near future.

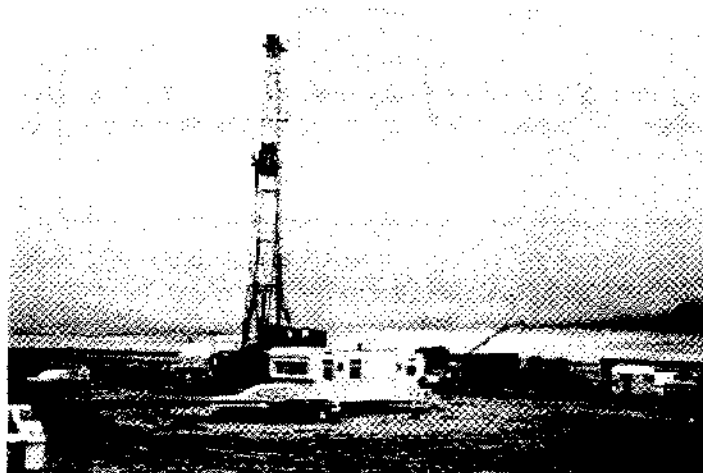


Figure 26. Preparatory operation of drilling and casing of test hole in potash formation.



Figure 27. Final checkup and zero calibration before placing creep-stress gage in test hole.

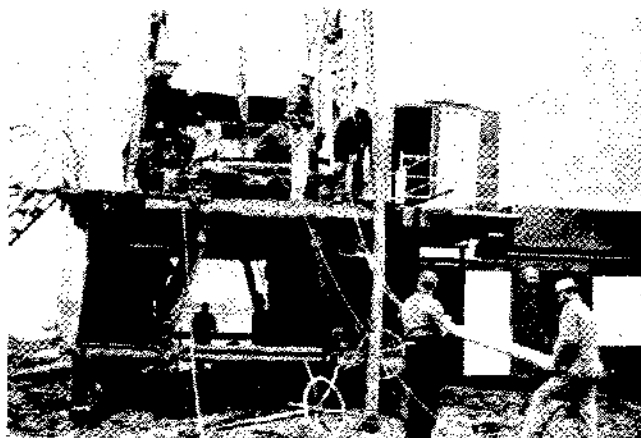


Figure 28. Placing of creep-stress gage by using drilling derrick.

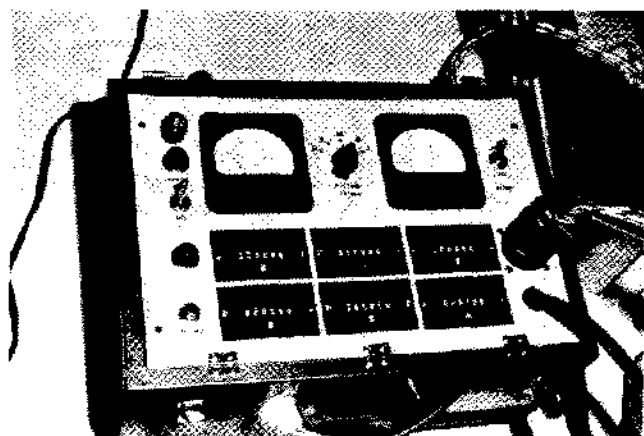


Figure 29. Remote control and readout unit operated on surface.

CONCLUSION

The following conclusions are drawn from the theoretical, laboratory, and field studies:

1. Salt mine structures generally contain two different states of the salt medium: nonconfined brittle state and confined ductile state. The geometric distribution of these two states in a salt mine structure determines its strength and behavior.
2. The creep behavior of a salt mine structure is determined mainly by the properties of the confined medium.
3. The behavior of ordinary salt mine structures cannot be calculated by mathematical means because of the presence of the two different states; however, it can be analyzed by using the laboratory model technique.
4. The laboratory model technique has been used successfully in the design of various salt mines, particularly for pillar size and shape, opening width and cross section, roof stability, and extraction rate of mining panel.
5. A creep-stress gage was developed to measure directly the stress condition of salt mine structures in situ. As the field tests are now in progress, the final results will be made available in the near future.

REFERENCES

1. K. Barron and N. A. Toews, 1963, Deformation around a mine shaft in salt: Internal Report FMP 63/29-MIN, Dept. of Mines and Technical Surveys, Ottawa.
2. A. M. Chowdiah, 1963, Stress and strain distribution around openings in underground salt formations: Ph.D. thesis, Dept. of Civil Engineering, Michigan State University.
3. R. Hill, 1960, The mathematical theory of plasticity: Clarendon Press, Oxford.
4. S. Serata, A. G. Dahir, and others, 1964, Principles of stress fields in underground formations: Progress Report No. 5 to National Science Foundation, Div. of Engineering Research, Michigan State University.
5. S. Serata and E. Gloyna, 1959, Development of design principles for disposal of reactor fuel waste into underground salt cavities: AEC Research Report No. TID-6317, Office of Technical Services, Dept. of Commerce, Washington 25, D. C.
6. S. Serata and E. Gloyna, 1960, Principle of structural stability of underground salt cavities: Journal of Geophysical Research, vol. 65, no. 9.
7. _____ and D. Morrison, 1962, The transition test as a method for determining the triaxial properties of rocks in the condition of underground formation: Progress Report No. 2 to National Science Foundation, Div. of Engineering Research, Michigan State University.
8. _____, 1961, Transition from elastic to plastic states of rocks under triaxial compression: Proceedings of 4th Symposium on Rock Mechanics, College of Mineral Industries, Pennsylvania State University.
9. _____, 1964, Theory and model of underground opening and support system: Proceedings of 6th Symposium on Rock Mechanics, University of Missouri at Rolla.
10. I. S. Sokolnikoff, 1956, Mathematical theory of elasticity: McGraw-Hill Company, New York.

ACKNOWLEDGMENT

The theoretical study and the laboratory work have been supported by the National Science Foundation, while the Canadian field work has been conducted as a joint project with Dr. William James of James, Cooper, and Buffam of Toronto. The creep-stress gage was built by Bendix System Division, Ann Arbor, Michigan.